Mathematical Biosciences and Engineering

MBE, 19(4): 4084–4100.
DOI: 10.3934/mbe.2022188
Received: 12 November 2021
Revised: 10 January 2022
Accepted: 08 February 2022
Published: 15 February 2022

http://www.aimspress.com/journal/MBE

Research article

Interlocked feedback loops balance the adaptive immune response

Lingli Zhou[1,2], Fengqing Fu[3,4], Yao Wang[1,2] and Ling Yang[1,2,*]

[1] School of Mathematical Sciences, Soochow University, Suzhou 215006, China
[2] Center for Systems Biology, Soochow University, Suzhou 215006, China
[3] Jiangsu Institute of Clinical Immunology, The First Affiliated Hospital of Soochow University, Suzhou 215000, China
[4] State Key Laboratory of Radiation Medicine and Protection, Soochow University, Suzhou 215123, China

* **Correspondence:** Email: lyang@suda.edu.cn; Tel: +8613913152842.

Abstract: Adaptive immune responses can be activated by harmful stimuli. Upon activation, a cascade of biochemical events ensues the proliferation and the differentiation of T cells, which can remove the stimuli and undergo cell death to maintain immune cell homeostasis. However, normal immune processes can be disrupted by certain dysregulations, leading to pathological responses, such as cytokine storms and immune escape. In this paper, a qualitative mathematical model, composed of key feedback loops within the immune system, was developed to study the dynamics of various response behaviors. First, simulation results of the model well reproduce the results of several immune response processes, particularly pathological immune responses. Next, we demonstrated how the interaction of positive and negative feedback loops leads to irreversible bistable, reversible bistable and monostable, which characterize different immune response processes: cytokine storm, normal immune response, immune escape. The stability analyses suggest that the switch-like behavior is the basis of rapid activation of the immune system, and a balance between positive and negative regulation loops is necessary to prevent pathological responses. Furthermore, we have shown how the treatment moves the system back to a healthy state from the pathological immune response. The bistable mechanism that revealed in this work is helpful to understand the dynamics of different immune response processes.

Keywords: immune response; cytokine storm; immune escape; mathematical model; bistable; feedback loops

1. Introduction

The adaptive immune response is a complex process that protects our body from external stimuli [1]. After infection with bacteria, viruses or parasites, naive T cells undergo a process of activation, proliferation and differentiation. These differentiated effector cells, especially Cytotoxic T lymphocytes (CTLs), are responsible for clearing pathogens. Once the pathogens are removed, the effector cells appear to be eliminated to maintain T cell homeostasis [2].

The immune system can discriminate between self and non-self, which depends on the precise control and regulation of immune cells, cytokines and signaling molecules. Kenneth introduced a detailed description of the immune response processes, which evolves from antigen presentation to effector immune defenses, and finally to the generation of immune memory [3]. Anisur reviewed the positive (negative) feedback loops (FLs) within the adaptive immune responses, and focuses on the influence of these interlocking loops on the efficient response [4]. In terms of pathological responses, Mok illustrated the potential mechanism by which systemic lupus erythematosus (SLE) develops from the point of immune dysregulation [5]. Some work has investigated the cellular and molecular mechanisms of immune escape in cancer, which also result from dysregulation of the immune system [6,7]. Therefore, both positive and negative FLs are important for the normal function of the immune system.

Mathematical modeling has proven to be a valuable tool to understand the immune system. In [8], the advantages of positive FLs are fully illustrated. Nicolas presented a conceptual mathematical model of autoimmune disease which is characterized by a positive FL [9]. Wang developed a HIV-immune model and analyzed the bistable response within the immune system [10]. Modeling studies on human hepatitis B virus (HBV) infection analyzed the relationship between HBV and the CTL-mediated immune response, and the simulation and theoretical results can interpret the wide range of clinical manifestations of HBV infection by taking different sets of parameters [11]. The role of negative FLs on immune response is also studied in some modeling work. Kalet well explained the tolerance of the immune system by a negative FL between Treg and effector T cells [12]. Given that transforming growth factor beta ($TGF-\beta$) functions as an inhibitory protein to effector immune cells, Mark analyzed the immunosuppressive mechanism induced by $TGF-\beta$ related negative feedback [13].

At the same time, tumor cells escape from immune-mediated destruction also attracted the attention to many scholars. Seyed described myeloid derived suppressor cells (MDSC) -induced immunosuppression mediated by tumor, which forms a positive FL between tumor and effector cells [14]. Lai has introduced PDE models with immune checkpoint proteins [15–18], and their studies focus on the efficacy of combinatorial inhibitor treatment for different cancer subtypes. These results are also consistent with clinical findings [19,20], in which the use of inhibitor therapy alone may lead to tumor hyper progression or cytokine storms.

There are also extensive studies on feedback mechanisms in immune system. Kormarova considered a two-dimensional ODE model (virus and immune cells) for antiviral immune response, and present a simple relation between timing of therapy and efficacy of drugs required for success [21]. Wodarz built an ODE framework to study oncolytic virus dynamics. They found that whether the viruses can eliminate the tumor depends on the replication rate of virus, which give potential implications beyond the study of virus therapy of cancers [22]. Lowengrub highlight the dynamic interaction of macrophages within a growing tumor, and showed that M2 cells lead to larger tumor growth through a modeling framework, which may help to optimize cancer immunotherapy [23]. All

these models give a detailed description about how immune system works to clear pathogens.

From the models mentioned above, we know that the FLs in immune system are responsible for a lot of diseases. However, some issues between biological behavior and modeling work remain unclear. For example, in an immune model with a positive FL, how to understand the hypersensitivity that occurs after the pathogen is eliminated, and why the immune system did not return to the healthy state of a bistable model. Furthermore, the regulatory effects of negative FLs on bistable model, especially the modeling of tumor immune escape behavior, also are not well studied. Based on these problems, we prefer to propose a model to explore the mechanism of hypersensitivity using irreversible bistability, and to understand the immune escape based on the role of negative FLs on bistability.

In this work, we develop a nonlinear model of the adaptive immune response. Compared with the existing models, the present model explains the mechanism of cytokine storm, which is induced by an irreversible bistability. The irreversibility results from ultra-strong positive feedbacks or ultra-weak negative feedbacks. What is more, we explain the mechanism of immune escape caused by ultra-strong negative feedbacks, which change the stability of the model from bistable to monostable. These mechanisms are also the novelties of the present model. The organization of the rest of the paper is as follows. Section II presents the mathematical model that describes infection-immune interactions. In section III, we outline the numerical simulation results which are qualitatively consistent with experimental results and theoretical analysis of the model. In this section, several pathological response behaviors will be reproduced, and the treatments for the pathological responses will also be discussed. We also compare the impact of different treatment methods and duration on the final outcome in this part. At last, section IV is a conclusion of the work.

2. Model formulation

2.1. Model description

Figure 1 is a schematic diagram illustrating the relationship between the infection and the immune system. The infected cells produce antigens, which are collected by dendritic cells. These dendritic cells interact with naive T cells, and activate them. Then, activated T cells secrete multiple cytokines, such as Interleukin-2 (IL-2), IL-6 and Interferon-γ (IFN-γ), which causes more naive T cells activation and proliferation. Upon expansion, activated T cells will differentiate into two cell types with different functions, namely CTLs and regulatory T cells (Tregs). The former releases cytotoxic cytokines to destroy infected cells, and the latter releases anti-inflammatory cytokines to inactivate the former. Furthermore, inhibitory protein production could also be indirectly promoted by CTLs to prevent overactivation of the immune system.

The infection-immune model in Figure 1 includes many regulatory FLs. There are two negative FLs and two positive FLs within the immune system, one of which is the self-promotion of activated T cells. If we consider the infected cells, one more negative feedback is present.

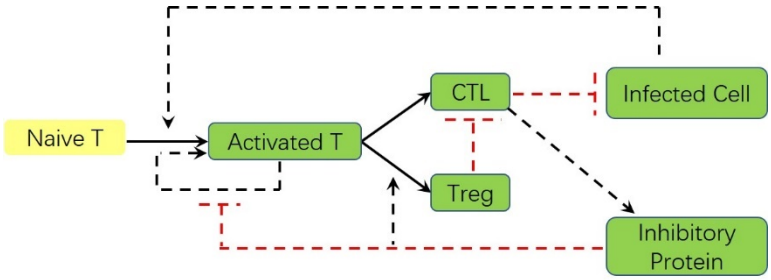

Figure 1. A diagram of immune response to infection. Dotted lines indicate positive (black) or negative (red) regulations, and solid line denote the transition between immune cells.

2.2. Model equation

The proposed mathematical model was developed utilizing five ordinary differential equations. Here we assume that the population of naive T cells is sufficient, and we only consider activated T cells, CTLs, Tregs, infected cells and inhibitory proteins as the model variables. In the absence of adequate experimental data, the model presented here is qualitative, not quantitative. The principles of model formulation include: the regulations result from realistic experimental data, and the model should reproduce the qualitative features of realistic immune response behavior. Specifically, we select arbitrary parameter values for which the model exhibits qualitative behaviors consistent with the normal response process. Equations of the five variables are show as follows:

$$\frac{dX}{dt} = \alpha \cdot \left(1 + \lambda \cdot \frac{C^2}{C^2 + {C_0}^2}\right) + K_1 \cdot \frac{X^2}{X^2 + {X_0}^2} \cdot \frac{{P_1}^2}{P^2 + {P_1}^2} - e_1 \cdot X - e_2 \cdot X \cdot \left(1 + \mu \cdot \frac{P}{P + P_2}\right) - d_X \cdot X \tag{1}$$

$$\frac{dY}{dt} = e_1 \cdot X - l_1 \cdot \frac{Z^2}{Z^2 + {Z_0}^2} \cdot Y - d_Y \cdot Y \tag{2}$$

$$\frac{dZ}{dt} = e_2 \cdot X \cdot \left(1 + \mu \cdot \frac{P}{P + P_2}\right) - d_Z \cdot Z \tag{3}$$

$$\frac{dC}{dt} = K_2 \cdot C \cdot \left(1 - \frac{C}{C_1}\right) \cdot \frac{C}{C + C_2} - l_2 \cdot Y \cdot C - d_C \cdot C \tag{4}$$

$$\frac{dP}{dt} = \beta * \frac{Y^2}{Y^2 + {Y_1}^2} - d_P \cdot P \tag{5}$$

Equation (1) describes the population of the activated T cells. The first term represents transformation of naive T cells to activated T cells due to infection [24,25], α, λ are the activation rate and maximum recruitment rate of infected cells to naive T cells. The second term describes the self-promotion of activated T cells [26–28], which can be suppressed by inhibitory proteins [20,29]. The third and fourth terms represent differentiation to CTLs and Tregs respectively. In addition, Treg differentiation could be facilitated by inhibitory proteins [30,31]. The last term is an apoptotic term.

Equation (2) gives the population of the CTLs. The first term is differentiation source of CTLs. The second term accounts for the reduction of CTLs by Tregs, due to the competition of IL-2 [32,33]. The last term $d_2 \cdot Y$ represents natural death.

Equation (3) gives the population of the Treg. $e_2 \cdot X \cdot (1 + \mu \cdot \frac{P}{P+P_2})$ is differentiation source of

Tregs, μ is the maximum promotion rate for Treg differentiation due to inhibitory proteins. $d_3 \cdot Z$ represents natural death.

Equation (4) models the population of the infected cells. It is assumed that infected cells follow a logistic growth formula with Allee effect, which could be indicated by the first term [34–36]. The second term in this equation describes elimination of infected cells by CTLs [37,38]. d_4 is the rate of normal cell death.

Equation (5) describes the population of the inhibitory proteins. We consider inhibitory proteins primarily produced by CTLs, this term explains the mechanism of immune system to prevent overactivation [39,40]. β in the first term is max production rate. $d_5 \cdot P$ describes protein degradation.

3. Results

3.1. Simulation for the normal immune response

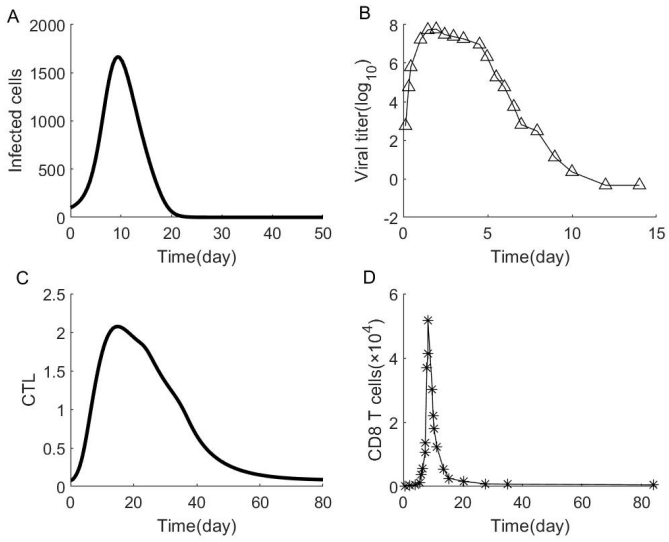

Figure 2. The normal immune response process (self-healing). Plots indicate the growth of infected cells (A) and immune cell populations (C) over time. Parameters values are taken from Table 1. In this case, the immune system is able to clear the infection. (B) and (D) show the normal immune response process: dynamics of the viral titer and the number of T cells.

We used our model to first mimic the normal immune response to infection, which is a self-healing process. As shown in Figure 2, the immune cells first undergo activation and expansion to clear infection, and then inactivation to return to their initially healthy levels. Initially, the immune system is in a healthy state, with infected cell populations varying from 0 to a large value (we take 100 here) after infection is present. In this case, the presence of infected cells induces the activation of naive T cells, so the population of activated T cells will expand, leading to the increase of CTL population in Figure 2C. Next, the population of Tregs will also increase due to differentiation of activated T cells. Since the population of CTLs at the early time is not sufficient to control the infection, infected cell populations will continue to increase. Until CTLs accumulate to a greater population to compete with infection, the population of infected cells will decrease because of killing by the CTLs.

To prevent overactivation of the immune system, inhibitory proteins induced by CTL down-regulate the response by promoting Tregs and suppressing activated T cells. This process allows the immune system to be inactivated and return back to the initial state once the infection is cleared.

Figure 2A,C show the normal immune response process by the model. Figure 2B,D shows the process of virus infection in experimental murine which are performed in vivo. The data points in these are shown by mean [41]. We connect adjacent data points with straight lines, to make it easy to explain a general trend. In the beginning, the population of immune cells are small. With the expanding of virus, the immune cells are activated and proliferates quickly to clear virus. When virus is eliminated, the population of immune cell will decrease to their original level. These figures depict a normal immune response process, which is also a process of activation first and then inactivation. Simulation results in Figure 2A,C are consistent qualitatively with the experimental results in Figure 2B,D.

Table 1. Parameters for Eqs (1)–(5).

Parameter	Definition	Value	Unit
α	Activation rate due to infection	0.01	arbitrary
λ	Maximum recruitment rate of naive T cells by infected cells	8	arbitrary
C_0	Half-saturation parameter for activation by infected cells	5	arbitrary
K_1	Maximum self-promotion rate of activated T cells	0.58	arbitrary
X_0	Half-saturation parameter for self-promotion of activated T cells	0.26	arbitrary
P_1	Half-saturation parameter due to inhibition by inhibitory proteins	1	arbitrary
e_1	Differentiation rate of CTLs	0.8	arbitrary
e_2	Differentiation rate of Tregs	0.2	arbitrary
μ	Maximum promotion rate of Treg differentiation due to inhibitory proteins	5	arbitrary
P_2	Half-saturation parameter for Treg differentiation due to promotion by inhibitory proteins	100	arbitrary
d_X	Death rate of activated T cells	0.1	arbitrary
l_1	CTL decrease rate due to inhibition by Tregs	2.5	arbitrary
Z_0	Half-saturation parameter for CTLs decreasing due to inhibition by Tregs	4	arbitrary
d_Y	Death rate of CTLs	0.1	arbitrary
d_Z	Death rate of Tregs	0.1	arbitrary
K_2	Proliferation rate of infected cells	1.2	arbitrary
C_1	Carry capacity of infected cells	9000	arbitrary
C_2	Allee constant	300	arbitrary
l_2	Decreasing rate of infected cell by CTLs	0.5	arbitrary
d_C	Death rate of infected cells	0.01	arbitrary
β	Maximum production rate for inhibitory proteins	3	arbitrary
Y_1	Half-saturation parameter for protein production due to CTLs	9	arbitrary
d_P	Degradation rate of inhibitory proteins	0.3	arbitrary

*Note: parameters of all simulations in the paper are taken from this table unless otherwise specified.

3.2. Simulation for pathological immune responses

This section presents three different types of pathological immune response processes under different immunological conditions, just as shown in Figure 3.

Figure 3A,B describe an immune response process in which infected cells proliferate with higher proliferation rate (K_2 changes from 1.2 to 2). During the first several days, infected cells in Figure 3A rapidly expand due to higher K_2. Additionally, immune cells will be activated, and begin competing with the infected cells. However, although infected cell populations decrease from 6th day, they will increase then and eventually maintain a high level. Because the infected cells cannot be eliminated all the time, the immune system will be continually activated. Figure 3A,B suggest that if the infected cells proliferate quickly, infected cells could proliferate rapidly within a short time. In this situation, the immune system cannot remove the infection on its own, which activate the immune system and results high levels of immune cytokines. Figure 3C shows the kinetics of TNF-a in the acute inflammatory response, which are performed on human lung tissue, in vitro [42]. Compared with control group, the concentration of TNF-a (cytokine that induces inflammation) maintains at a significantly high level in the lipopolysaccharide (LPS) stimulated tissue.

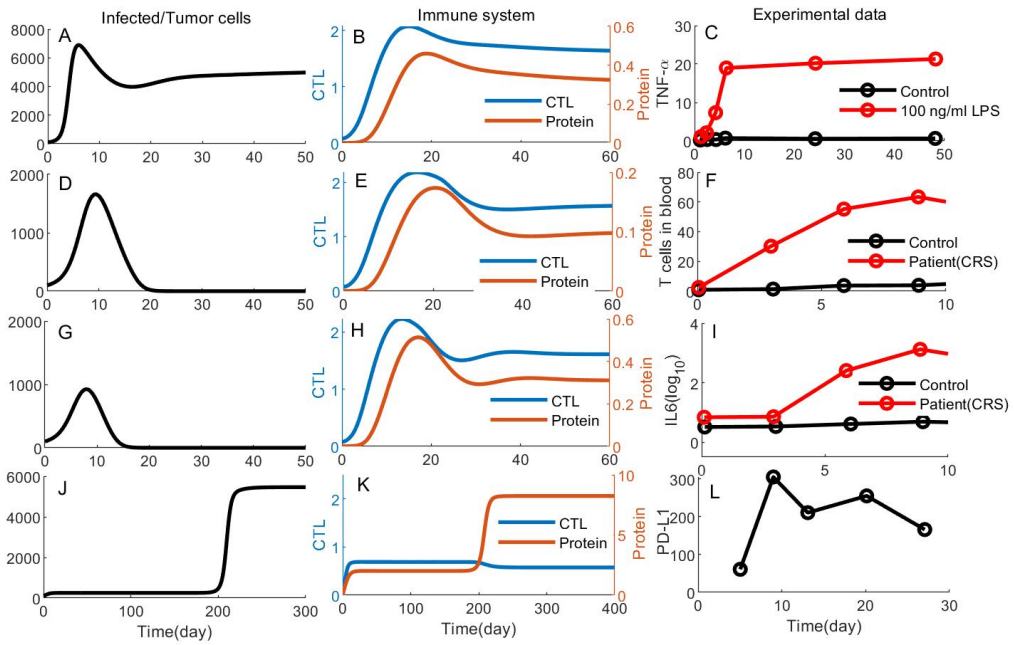

Figure 3. Pathological responses of the model and several experimental results. Left and center columns relate to model results, including the immune response to infection (A&B&D&E&G&H), and to tumor cells (J&K). In detail, immune response in (A&B) corresponds a fast proliferation of infected cells ($K_2 = 2$). For (D&E), the immune system has a low production rate of inhibitory proteins ($\beta = 1$). A high self-promotion rate ($K_1 = 0.65$) of activated T cells is considered in (G-H). Right column gives several immunological responses from experiments: (C) describes the dynamics of TNF-a in acute inflammation response. (F&I) show dynamical population of T cells and IL-6 in control group and patients after CAR-T therapy. (L) describes the dynamics of PD-L1 in mouse immune cells.

In contrast to Figure 2, the populations of immune cells in Figure 3C cannot return to their initial levels after the infection has been cleared. Because of the lower production rate of inhibitory proteins,

the populations of activated T cells and Tregs are not to be downregulated.

Figure 3D,E are consistent with the characteristics of cytokine release syndrome (CRS) or cytokine storm, suggesting that negative feedback is associated with CRS. In the absence of negative feedback or the negative feedback is weak, the immune system could remove the infection, but it cannot return to its healthy state and a complete immune response process cannot be achieved. Cytokine storms will cause destruction to multiple normal organs.

Figure 3G,H can also capture the characteristics of cytokine storms, which results from the strong positive feedback induced by larger K_1. Compared with Figure 3D,E, Figure 3G,H suggest that even if the production rate of inhibitory proteins (β) is moderate, if the self-promotion of activate T cells is very strong, immune cell populations will remain at a high level after the infection is eliminated.

Figure 3G,H show that both higher self-promotion rate of activated T cells and lower production rate of inhibitory proteins in the model could replicate the features of cytokine storms. This figure suggests that there should be a balance between activation and inhibition during the normal immune response. If the activation is ultra-strong or the inhibition is ultra-weak, the immune system will not be inactivated to its healthy state after the infection is cleared, and will remain activated forever. Figure 3F,I give the concentrations of immune cells and cytokines in serum obtained from patients, which are performed in vivo, and patients maintain a high level of cytokines and immune cells after CAR-T therapy [43].

Tumor development is closely related to the immune system, so we consider a long-term immune response process in our model. Compared to the infection model, tumor cells can prevent attacks from the immune cells by a number of mechanisms [7,44,45], including the overexpression of inhibitory immune checkpoint molecules (e.g., PD-1, CTLA-4, Tim-3). Take the coinhibitory immune complex PD-1/PD-L1 as an example. Tumor cells are capable of overexpressing the membrane protein PD-L1, and the binding of PD-L1 and PD-1 blocks the proliferation of activated T cells and contributes to Treg differentiation [30,46]. The mechanism of tumor immune escape by PD-1/PD-L1 suggests there is a positive regulation of tumor cells to inhibitory proteins production. It's to say, one additional regulation should be added to Eq (5) for this model, which is shown below,

$$\frac{dP}{dt} = \beta * \frac{Y^2}{Y^2 + {Y_1}^2} + K_3 \cdot \frac{C}{C + C_3} - d_P \cdot P \tag{6}$$

In Figure 3J, the population of tumor cells gradually accumulates at an early stage. Once the population increases to a critical level, the ultra-strong inhibition induced by the second term $K_3 \cdot \frac{C}{C+C_3}$ of Eq (6) is activated, which leads to the suppression of activated T cells and ultimately contributes to the proliferation of tumor cells. There are two features of this immune response: one is that tumor cells cannot be removed due to the addition of inhibitory proteins, the other is that the population of tumor cells cannot increase rapidly due to early accumulation.

Figure 3J,K demonstrate that by adding the above regulation, the time required for tumor to grow into a pathological population is prolonged. During this period, the tumor and the immune system are in a gaming state. Compared to Figure 2, the results in Figure 3J,K show that it's the added regulation that helps tumor to escape from immune cell-mediated destruction. Figure 3J,K are consistent qualitatively with the experimental results shown in Figure 3L, in which PD-L1 is greatly expressed for a long time in mice bearing T9 sarcoma cells [47].

Our mathematical model well reproduces several different immune response processes (Figure 3).

For these processes, there are obvious differences between normal responses and pathological responses, and these mechanisms are not clear.

3.3. Dynamical analysis

Our earlier model includes the FLs between two components (infection and immune system). In order to determine the mechanism of different response behaviors within the immune system, we view the infection as a constant stimulus to the immune system in the following section. The reduced model developed here opens up the closed loop between the immune system and the stimulus. Figure 4 is a reduced model including a constant stimulus, and retain the FLs inside the immune system.

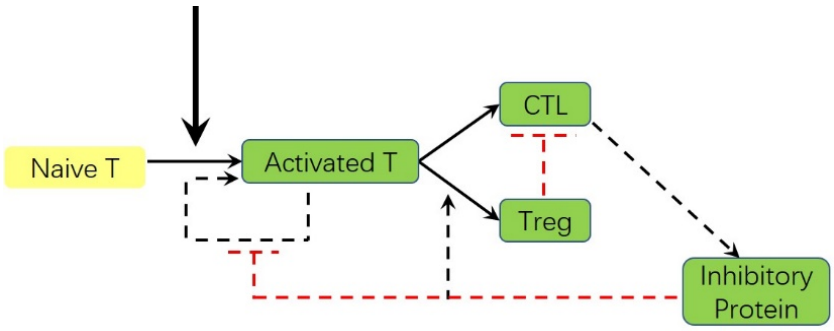

Figure 4. A diagram of immune response to a constant antigen stimulus. The thick and black line is a constant stimulus. Dotted lines indicate positive (black) or negative (red) regulation, and solid line denote the transformation between immune cells.

Equations of the four variables corresponding to the Figure 4 are show as follows:

$$\frac{dX}{dt} = s + K_1 \cdot \frac{X^2}{X^2+{X_0}^2} \cdot \frac{{P_1}^2}{P^2+{P_1}^2} - e_1 \cdot X - e_2 \cdot X \cdot \left(1 + \mu \cdot \frac{P}{P+P_2}\right) - d_X \cdot X \tag{7}$$

$$\frac{dY}{dt} = e_1 \cdot X - l_1 \cdot \frac{Z^2}{Z^2+{Z_0}^2} \cdot Y - d_Y \cdot Y \tag{8}$$

$$\frac{dZ}{dt} = e_2 \cdot X \cdot \left(1 + \mu \cdot \frac{P}{P+P_2}\right) - d_Z \cdot Z \tag{9}$$

$$\frac{dP}{dt} = \beta * \frac{Y^2}{Y^2+{Y_1}^2} - d_P \tag{10}$$

Figure 5 shows the steady production of the CTLs as a function of the constant stimulus s under different K_1 and β. K_1 is the self-promotion rate of activated T cells, which determines the strength of positive feedback in Figure 4. β is the production rate of inhibitory proteins by CTLs.

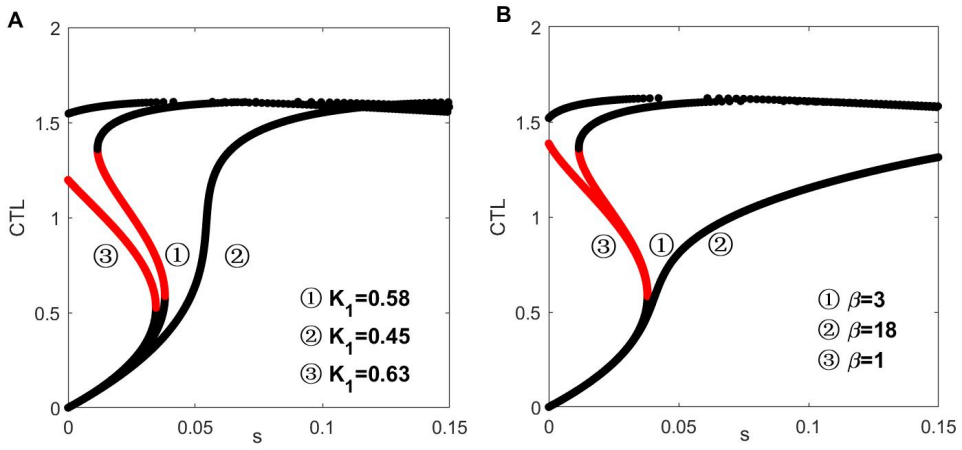

Figure 5. System's multi-stable response under different positive and negative regulations. (A) Bifurcation results under different self-promotion rate of activated T cells. (B) Bifurcation results under different production rate of inhibitory proteins. Black lines indicate stable steady points, red lines indicate unstable steady points. For both panels: ① reversible and bistable, ② monostable, ③ irreversible and bistable.

The bifurcation line ① (both in Figure 5A,B) is the control cases (normal situation), in which $K_1 = 0.45, \beta = 3$. For one healthy individual, $s = 0$ and $Y(CTL) = 0$. As s increases from 0, so does the stable population of CTLs. Once s increases to pass a critical value (≈ 0.03806), the system loses its lower branch, and the CTLs population jumps up to the upper branch. This means that once the infection reaches a critical population, the immune system initiates a strong response. Then, the immune system suppresses the infection and s decreases. Once s is reduced to a critical value (≈ 0.01157), the system loses its upper branch, and the CTLs jumps down to the lower branch. In this way, the immune system is able to eliminate the infection. This process characterizes the mechanism of normal immune response process.

If K_1 is greater than the control value of Figure 5A, the bistable switch become irreversible. This means that after jumping up to the upper branch of line ②, even if the activated immune system could clear the stimulation, the population of immune cells still remains a much high level. This case is consistent with the immune response observed in Figure 3D,E and Figure 3G,H.

If K_1 is lower than the control value of Figure 5A, the bistable switch become monostable. In this case, small K_1 induces a weak FL that cannot guarantee bistability. The corresponding immune response cannot achieve a switch-like behavior.

Because the inhibitory proteins directly suppress the FL, altering β (Figure 5B) will lead to the change of steady states, which is opposite to the change of K_1. In the previous infection model (nonconstant), the pathological responses (cytokine storms) in Figure 3D,E and Figure 3G,H correspond to irreversible bistability ③ in Figure 5B and Figure 5A respectively. The pathological responses process (tumor immune escape) in Figure 3G,H corresponds to ② in Figure 5B. In the section below, we will present the treatment for these pathological immune responses.

3.4. Drug treatments

3.4.1. Treatment for pathological response with greater K_2

The immune response to a common infection follows a switch-like behavior (Figure 5①). In infected cells with high proliferation rates, the immune response begins with a jump to the upper branch of the switch, but the jumping down behavior is absent because the immune system is unable to decrease the stimulus s. In this case, antibiotics or other drugs are necessary to complete the normal immune response.

Antibiotics are often used to treat bacterial infections. Some antibiotics reduce the growth rate of bacteria by interfering with their DNA replication, and some antibiotics increase their mortality by inhibiting the synthesis of cell walls. Therefore, we can use two intervention methods to mimic the antibiotics treatment (decrease K_2 and increase d_c). The details are show in the following figure:

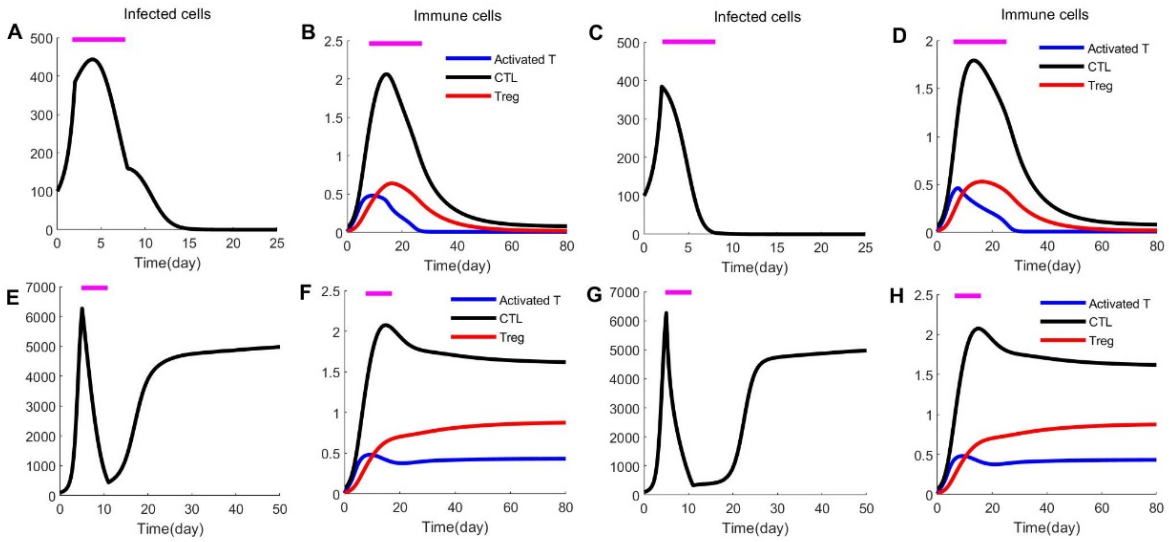

Figure 6. Simulations for the antibiotic treatments. Medication duration for the upper panel (A&B&E&F) is from 2th day to 8th day, while lower panel (E&F&G&H) is from 5th day to 11th day. Drug target of (A&B&E&F) is the proliferation rate, while (C&D&G&H) is the death rate. The length of pink lines at the top of each subfigure represents the duration of the medication.

As shown in Figure 6A–D, both decreasing K_2 (from 0.8 to 0.4) and increasing d_c (from 0.01 to 1.05) can eliminate the infection, and eventually the population of immune cells decreases to its original level. However, if we postpone the onset of treatment in Figure 6E–H, although the infected cell population decreases to a much lower level, it will increase and maintain a high level once we stop the treatments. This figure indicates that the time to start treatment is also important to clear infections.

3.4.2. Treatment for cytokine storm

Cytokine storm is a systemic inflammatory syndrome, and will result in increased levels of cytokines and overactivation of the immune system. During the adaptive immune response (Figure 1), the activated immune cells secrete cytokines to activate more naive immune cells. This process is a

key positive feedback loop, which rapidly initiates the immune response.

However, an abnormal and uncontrolled production of cytokines has been observed in some diseases, such as cytokine release syndrome after CAR-T therapy, arthritis (RA) and SLE. In these two diseases, an invader (bacteria or virus) triggers an immune response and leaves antibodies in the body. However, these antibodies may not be unique enough so that the immune system initiates the immune response to autoantibodies, and this induces high populations of immune cells and cytokines.

Glucocorticoid therapy is widely used to treat diseases caused by hypersensitivity. These diseases are similar to the immune response behavior in Figure 3C–F, in which the infection is removed and the population of the immune cells retains high. Glucocorticoids reduce the rate of cytokine production, and attenuate the FL. Once it reaches a critical value, the bistability of the system is changed from irreversible to reversible, which corresponds to the Figure 2. After the infection is removed, immune cells and cytokines will return back to their healthy levels.

In our model, the cytokine production rate is determined by K_1, so we can reduce K_1 to mimic the glucocorticoid treatment. Whether the cytokine storm is caused by an ultra-strong positive FL or an ultraweak negative FL, it can be cured by glucocorticoids as shown in Figure 7. Given the multiple side effects, it is necessary to pay more attention to the dose and duration of glucocorticoid treatment.

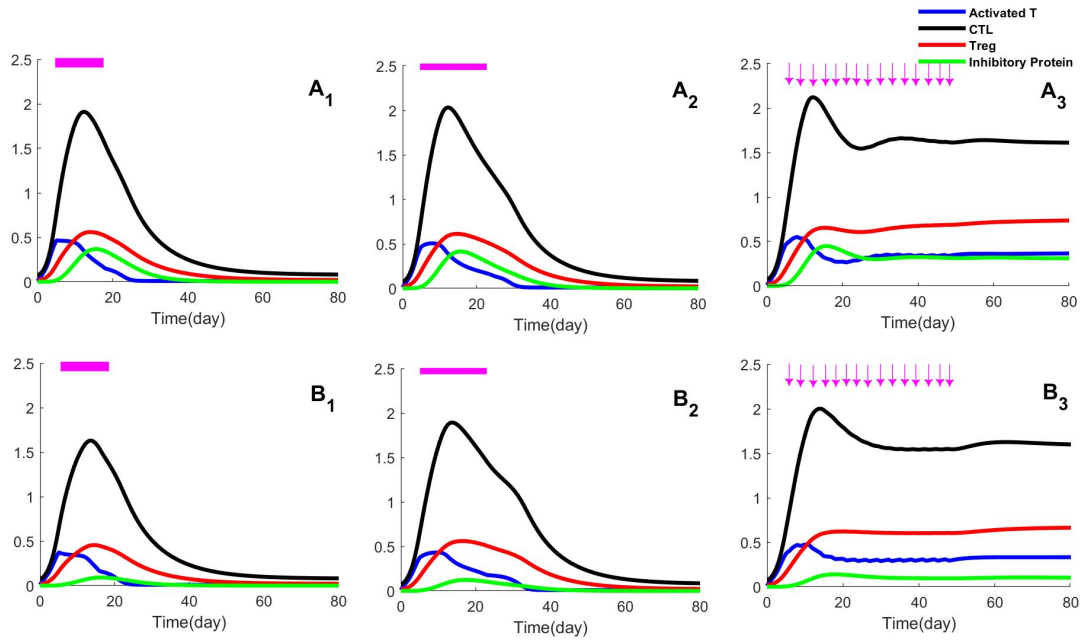

Figure 7. Simulation of glucocorticoid treatment. Panel (A) and (B) are treatments of cytokine storms induced by larger K_1 and smaller β. Every subpanel indicates a different administration proposal. The length of pink line at the top of each subfigure represents the duration of the medication, while the height represents the dose of the medication.

Figure 7A_1,B_1 refer to large dose of glucocorticoids, and after 13 and 11 days of maintenance medication, immune cell populations can all drop to their original and normal levels. Figure 7A_2,B_2 refer to moderate dose, and after 20 and 18 days of maintenance medication, immune cell populations also decrease to their original levels. Figure 7A_3,B_3 refer to small doses and intermittent medication for 45 days, while immune cell populations remain at high levels indefinitely.

Figure 7 indicates that the dose and duration of medication are two critical factors in the treatment

of cytokine storms. Clinically, developing an individualized medication proposal based on the patient will be the best way to prevent the side effects of glucocorticoid.

3.4.3. Treatment for tumor immune escape

Tumor cells can escape anti-tumor immune responses through numerous mechanisms, one of which is the over-expression of coinhibitory membrane proteins, such as the immune-checkpoint molecule PD-L1. Immune-checkpoint therapy aims to block PD-1 binding with PD-L1, and this therapy has proven effective for some cancers.

For the tumor immune escape in our model (Figure 3G,H), the steady state is changed from ① to ② in Figure 5B, so an efficient removal process cannot be initiated. By introducing PD-1 inhibitors, the pathway between tumor cells and inhibitory proteins is inhibited, and the steady state returns to the healthy state.

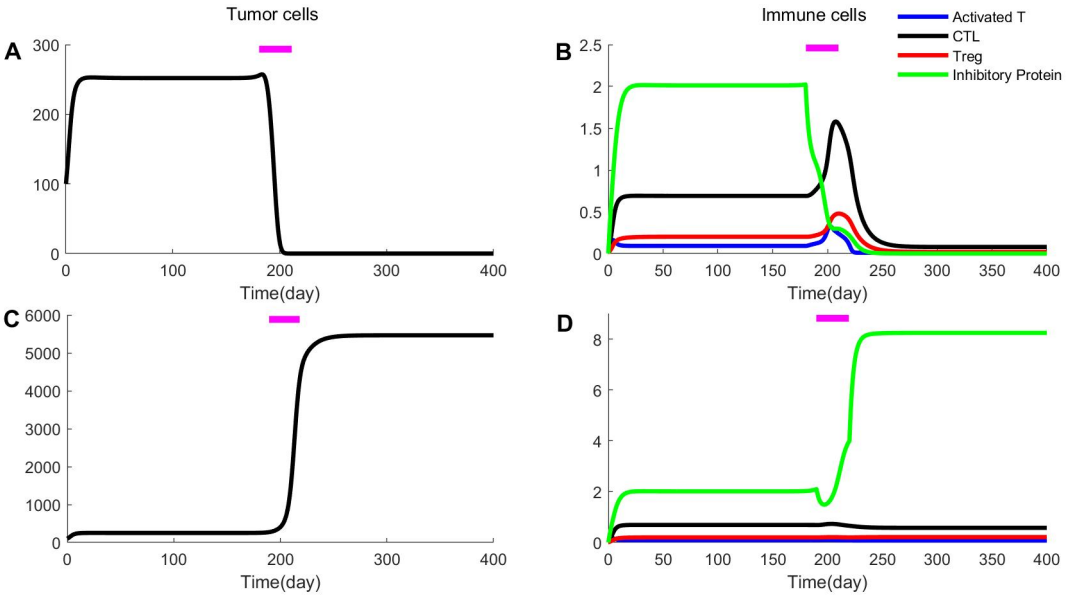

Figure 8. Simulation of immune checkpoint inhibitor treatment. Treatments identify the production rate of inhibitory protein by tumor cells as a drug target under different time to start the medication. Medication duration for the upper panel (A&B) is 180^{th}–210^{th} day, while lower panel (C&D) is 190^{th}–220^{th} day, The length of pink line at the top of each subfigure represents the duration of the medication.

In our tumor model (Figure 6), this treatment could suppress the production of inhibitory proteins that are promoted by tumor cells. To mimic the PD-1 inhibitor treatment, we decrease K_3 to half to initiate the immune response. When the treatment begins earlier (Figure 8A,B), immune cells can be greatly activated, and then tumor cells can be cleared. However, if the treatment is initiated 10 days later (Figure 8C,D), immune cells can only be activated to a small extent, and tumor cell populations rapidly increase to high levels. This figure suggests it's better to take medicine at an earlier time for tumor treatment.

4. Conclusions

The immune response is a complex process, and this process involves the regulation of different immune cells, signaling molecules and cytokines via positive or negative FLs. FLs have been shown to play a crucial role in shaping an efficient immune response. In this work, we propose a qualitative mathematical model to explain the different immune response behaviors, especially the pathological immune responses.

Our model incorporates one positive FL and two negative FLs within the immune system, and the modeling principle is based on the biological regulations. When the immune system encounters a foreign antigen, immune cells become activated and expand quickly, which characterized by a switch-like behavior mediated by positive FLs. In order to maintain self-tolerance, the immune system develops negative FLs, and the immune cells are attenuated or switched off to retain homeostasis after the antigen is removed.

The immune system's switch-like behavior can be reproduced by our model, and this behavior presents a normal immune response process. However, many diseases are caused by pathological immune responses. For some autoimmune diseases accompanied by the overactivation of the immune system, our model with high (low) strength of positive (negative) FL could replicate these disease progressions. Simulations show that immune cell populations do not fall back to their initial levels when infection was eliminated, which is consistent with experimental data. In this case, the immune system alone is not fully effective against the progression of infection, additional drug treatments, such as immunosuppressive drugs, can help to achieve the switch-like behavior again. During tumor development, studies have found multiple mechanisms of immune escape in the tumor immune cycle. We modeled the effects of PD-L1 overexpression on tumor progression, and found that this overexpression weakens the negative feedback of the model, which leads to the absence of switch-like behavior either. Bifurcation analysis of reduced model illustrates that any abnormal positive (negative) FLs lead to a pathological immune response. A normal and efficient switch-like response results from a balance between positive FLs and negative FLs.

In conclusion, the present study proposes an ODE-based mathematical model of immune responses. The model could reproduce several different pathological responses, which result from the imbalance between FLs. Our model and results are useful for understanding of immune system behaviors.

Acknowledgements

This study is supported by the National Key Research and Development Program of China (2018YFA0801103), the National Natural Science Foundation of China (12071330) to Prof. Ling Yang, and China Scholarship Council and Post graduate Research. The authors would like to thank the reviewers and the editors for their valuable suggestions.

Conflict of interest

All authors declare no conflicts of interest in this paper.

References

1. C. A. Janeway, How the immune system works to protect the host from infection: A personal view, *Proc. Natl. Acad. Sci*., **98** (2001), 7461–7468. https://doi.org/10.1073/pnas.131202998
2. R. D. Michalek, J. C. Rathmell, The metabolic life and times of a T-cell, *Immunol. Rev.*, **236** (2010), 190–202. https://doi.org/10.1111/j.1600-065X.2010.00911.x
3. K. C. Mccullough, A. Summerfield, Basic concepts of immune response and defense development, *ILAR J.*, **46** (2005), 230–240. https://doi.org/10.1093/ilar.46.3.230
4. A. Rahman, A. Tiwari, J. Narula, T. Hickling, Importance of feedback and feedforward loops to adaptive immune response modeling, *CPT: Pharmacometrics Syst. Pharmacol.*, **7** (2018), 621–628. https://doi.org/10.1002/psp4.12352
5. C. C. Mok, C. S. Lau, Pathogenesis of systemic lupus erythematosus, *J. Clin. Pathol.*, **56** (2003), 481–490. https://doi.org/10.1136/jcp.56.7.481
6. A. Bhatia, Y. Kumar, Cellular and molecular mechanisms in cancer immune escape: a comprehensive review, *Expert Rev. Clin. Immunol.*, **10** (2013), 41–62. https://doi.org/10.1586/1744666X.2014.865519
7. D. S. Vinay, E. P. Ryan, G. Pawelec, W. H. Tallib, J. Stagg, E. Elkord, et al., Immune evasion in cancer: Mechanistic basis and therapeutic strategies, *Semin. Cancer Biol.*, **35** (2015), 185–198. https://doi.org/10.1016/j.semcancer.2015.03.004
8. K. A. Abdel-Sater, Physiological positive feedback mechanisms, *Am. J. Biomed. Sci.*, **3** (2011), 145–155. https://doi.org/10.5099/aj110200145
9. N. Rapin, E. Mosekilde, O. Lund, Bistability in autoimmune diseases, *Autoimmunity*, **44** (2011), 256–260. https://doi.org/10.3109/08916934.2010.523233
10. S. Wang, F. Xu F, L. Rong, Bistability analysis of an HIV model with immune response, *J. Biol. Syst.*, **25** (2017), 677–695. https://doi.org/10.1142/S021833901740006X
11. C. Long, H. Qi, S. Huang, Mathematical modeling of cytotoxic lymphocyte-mediated immune response to hepatitis B virus infection, *J. Biomed. Biotechnol.*, **2008** (2008), 743690. https://doi.org/10.1155/2008/743690
12. K. León, A. Lage, J. Carneiro, Tolerance and immunity in a mathematical model of T-cell mediated suppression, *J. Theor. Biol.*, **225** (2003), 107–126. https://doi.org/10.1016/S0022-5193(03)00226-1
13. M. Robertson-Tessi, A. El-Kareh, A. Goriely, A mathematical model of tumor-immune interactions, *J. Theor. Biol.*, **294** (2011), 56–73. https://doi.org/10.1016/j.jtbi.2011.10.027
14. M. A. Vogelbaum, B. Otvos, B. Raychaudhuri, D. Hambardzumyan, J. Finke, J. Lathia, The role of Myeloid derived suppressor cells (MDSCs) in tumor-induced immunosuppression in human and murine gliomas, *Neuro-Oncology*, **16** (2014), 44–44. https://doi.org/10.1093/neuonc/nou209.10
15. X. Lai, A. Stiff, M. Duggan, R. Wesolowski, W. E. Carson III, A. Friedman, Modeling combination therapy for breast cancer with BET and immune checkpoint inhibitors, *Proc. Natl. Acad. Sci.*, **115** (2018), 5534–5539. https://doi.org/10.1073/pnas.1721559115
16. X. Lai, A. Friedman, How to schedule VEGF and PD-1 inhibitors in combination cancer therapy, *BMC Syst. Biol.*, **13** (2019), 30. https://doi.org/10.1186/s12918-019-0706-y
17. X. L. Lai, A. Friedman, Combination therapy for melanoma with BRAF/MEK inhibitor and immune checkpoint inhibitor: a mathematical model, *BMC Syst. Biol.*, **11** (2017), 70. https://doi.org/10.1186/s12918-017-0446-9

18. A. Friedman, X. Lai, Combination therapy for cancer with oncolytic virus and checkpoint inhibitor: A mathematical model, *PLoS ONE*, **13** (2018), e0192449. https://doi.org/10.1371/journal.pone.0192449
19. T. Kamada, Y. Togasjhi, C. Tay, D. Ha, A. Sasaki, Y. Nakamura, et al., PD-1+ regulatory T cells amplified by PD-1 blockade promote hyperprogression of cancer, *Proc. Natl. Acad. Sci.*, **116** (2019), 9999–10008. https://doi.org/10.1073/pnas.1822001116
20. S. J. Rotz, D. Leino, S. Szabo, J. L. Mangino, B. K. Turpin, J. G. Pressey, Severe cytokine release syndrome in a patient receiving PD-1-directed therapy, *Pediatr. Blood Cancer*, **64** (2017), e26642. https://doi.org/10.1002/pbc.26642
21. N. L. Komarova, E. Barnes, P. Klenerman, D. Wodarz, Boosting immunity by antiviral drug therapy: A simple relationship among timing, efficacy, and success, *Proc. Natl. Acad. Sci.,*, **100** (2003), 1855–1860. https://doi.org/10.1073/pnas.0337483100
22. N. L. Komarova, D. Wodarz, ODE models for oncolytic virus dynamics, *J. Theor. Biol.*, **263** (2010), 530–543. https://doi.org/10.1016/j.jtbi.2010.01.009
23. G. Mahlbacher, L. T. Curtis, J. Lowengrub, H. B. Frieboes, Mathematical modeling of tumor-associated macrophage interactions with the cancer microenvironment, *J. Immunother. Cancer*, **6** (2018), 10. https://doi.org/10.1186/s40425-017-0313-7
24. L. J. Carreno, P. A. González, A. M. Kalergis, Modulation of T cell function by TCR/pMHC binding kinetics, *Immunobiology*, **211** (2006), 47–64. https://doi.org/10.1016/j.imbio.2005.09.003
25. K. Li, R. William, Z. Yuan, C. Zhu, Single-molecule investigations of T-cell activation, *Curr. Opin. Biomed. Eng.*, **12** (2019), 102–110. https://doi.org/10.1016/j.cobme.2019.10.005
26. P. Rozman, U. Svajger, The tolerogenic role of IFN-γ, *Cytokine Growth Factor Rev.*, **41** (2018), 40–53. https://doi.org/10.1016/j.cytogfr.2018.04.001
27. J. D. Burke, H. A. Young, IFN-γ: A cytokine at the right time, is in the right place, *Semin. Immunol.*, **43** (2019), 101280. https://doi.org/10.1016/j.smim.2019.05.002
28. J. H. Esensten, Y. A. Helou, G. Chopra, A. Weiss, J. A. Bluestone, CD28 costimulation: from mechanism to therapy, *Immunity*, **44** (2016), 973–988. https://doi.org/10.1016/j.immuni.2016.04.020.
29. M. Mandai, J. Hamamishi, K. Abiko, N. Matsumura, T. Baba, I. Konnishi, Dual faces of IFNγ in cancer progression: a role of PD-L1 induction in the determination of pro-and antitumor immunity, *Clin. Cancer Res.*, **22** (2016), 2329–2334. https://doi.org/10.1158/1078-0432.CCR-16-0224
30. L. M. Francisco, V. H. Salinas, K. E. Brown, V. K. Vangugri, G. J. Freeman, V. K. Kuchroo, et al., PD-L1 regulates the development, maintenance, and function of induced regulatory T cells, *J. Exp. Med.*, **206** (2009), 3015–3029. https://doi.org/10.1084/jem.20090847
31. E. Batlle, J. Massagué, Transforming growth factor-β signaling in immunity and cancer, *Immunity*, **50** (2019), 924–940. https://doi.org/10.1016/j.immuni.2019.03.024
32. P. Pandiyan, L. Zheng, S. Ishiharam, J. Reed, M. J. Lenardo, CD4+CD25+Foxp3+ regulatory T cells induce cytokine deprivation-mediated apoptosis of effector CD4+ T cells, *Nat. Immunol.*, **8** (2007), 1353–1362. https://doi.org/10.1038/ni1536
33. P. Trzonkowski, E. Szmit, J. Myliwska, A. Mysliwski, CD4+CD25+ T regulatory cells inhibit cytotoxic activity of CTL and NK cells in humans-impact of immunosenescence, *Clin. Immunol.*, **119** (2006), 307–316. https://doi.org/10.1016/j.clim.2006.02.002
34. L. Sewalt, K. Harley, P. V. Heijster, S. Balasuriya, Influences of Allee effects in the spreading of malignant tumours, *J. Theor. Biol.*, **394** (2016), 77–92. https://doi.org/10.1016/j.jtbi.2015.12.024

35. Y. V. Tyutyunov, S. Sen, L. I. Titova, M. Banerjee, Predator overcomes the Allee effect due to indirect prey-taxis, *Ecol. Complexity*, **39** (2019), 100772. https://doi.org/10.1016/j.ecocom.2019.100772
36. Y. Yu, J. J. Nieto, A. Torres, K. Wang, A viral infection model with a nonlinear infection rate, *Boundary Value Probl.*, **2009** (2009), 958016. https://doi.org/10.1155/2009/958016
37. S. Halle, O. Halle, R. Förster, Mechanisms and dynamics of T cell-mediated cytotoxicity in vivo, *Trends Immunol.*, **38** (2017), 432–443. https://doi.org/10.1016/j.it.2017.04.002
38. B. Weigelin, M. Krause, P. Friedl, Cytotoxic T lymphocyte migration and effector function in the tumor microenvironment, *Immunol. Lett.*, **138** (2011), 19–21. https://doi.org/10.1016/j.imlet.2011.02.016
39. J. R. Schoenborn, C. B. Wilson, Regulation of interferon-gamma during innate and adaptive immune responses, *Adv. Immunol.*, **96** (2007), 41. https://doi.org/10.1016/S0065-2776(07)96002-2
40. K. Abiko, N. Matsumura, J. Hamanishi, N. Horikawa, R. Murakami, K. Yamaguchi, et al., IFN-γ from lymphocytes induces PD-L1 expression and promotes progression of ovarian cancer, *Br. J. Cancer*, **112** (2015), 1501–1509. https://doi.org/10.1038/bjc.2015.101
41. H. Miao, J. A. Hollenbaugh, M. S. Zand, J. Holden-Wiltse, T. R. Mosmann, A. S. Perelson, et al., Quantifying the early immune response and adaptive immune response kinetics in mice infected with influenza A virus, *J. Virol.*, **13** (2010), 6687–6698. https://doi.org/10.1128/JVI.00266-10
42. T. L. Hackett, R. Holloway, S. T. Holgate, J. A. Warner, Dynamics of pro-inflammatory and anti-inflammatory cytokine release during acute inflammation in chronic obstructive pulmonary disease: an ex vivo study, *Respir Res.*, **9** (2008), 47. https://doi.org/10.1186/1465-9921-9-47
43. K. A. Hay, L. A. Hanafi, D. Li, J. Gust, W. C. Liles, M. M. Wurfel, et al., Kinetics and biomarkers of severe cytokine release syndrome after CD19 chimeric antigen receptor-modified T-cell therapy, *Blood*, **130** (2017), 2295–2306. https://doi.org/10.1182/blood-2017-06-793141
44. X. Jiang, J, Wang, X. Deng, F. Xiong, J. Ge, B. Xiang, et al., Role of the tumor microenvironment in PD-L1/PD-1-mediated tumor immune escape, *Mol. Cancer*, **18** (2019), 10. https://doi.org/10.1186/s12943-018-0928-4.
45. H. Dong, S. E. Strome, D. R. Salomao, H. Tamura, F. Hirano, D. B. Flies, et al., Tumor-associated B7-H1 promotes T-cell apoptosis: A potential mechanism of immune evasion, *Nat. Med.*, **8** (2002), 793–800. https://doi.org/10.1038/nm730
46. N. Patsoukis, J. Brown, V. Petkova, F. Liu, L. Li, V. A Boussiotis, Selective effects of PD-1 on Akt and Ras pathways regulate molecular components of the cell cycle and inhibit T cell proliferation, *Sci. Signaling*, **5** (2012). https://doi.org/10.1126/scisignal.2002796
47. T. Noguchi, J. P. Ward, M. M. Gubin, C. D. Arthur, S. H. Lee, J. Hundal, et al., Temporally distinct PD-L1 expression by tumor and host cells contributes to immune escape, *Cancer Immunol. Res.*, **5** (2017), 106–117. https://doi.org/10.1158/2326-6066.CIR-16-0391

AIMS Press